Preparation of an ordered ultra-thin aluminosilicate framework composed of hexagonal prisms forming a percolated network

J. Anibal Boscoboinik*[,a], Xin Yu [a], Shamil Shaikhutdinov [a] and Hans-Joachim Freund [a]

[a] Fritz-Haber-Institut der Max-Planck-Gesellschaft, Faradayweg 4 - 6, 14195 Berlin, Germany.

* Corresponding Author. Tel.: +49 30 8413 4218, Fax: +49 30 8413 4101, email address: bosco@fhi-berlin.mpg.de.

ABSTRACT: A flat ultra-thin (0.5 nm thick) aluminosilicate framework was grown using Ru(0001) as a template. The structure and composition were determined by a combination of scanning tunneling microscopy, low energy electron diffraction, infrared reflection absorption spectroscopy and x-ray photoelectron spectroscopy experiments. This film is composed mainly of an ordered arrangement of double six-membered rings *d6r* (a.k.a. hexagonal prisms) and it covers ~ 45% of the surface, forming a two-dimensional percolated network. The remaining "uncovered" area leaves the Ru(0001) surface exposed through irregularly shaped holes of sizes in the mesopore scale range. The film morphology is different from that observed for pure silica, where a monolayer structure bound to the Ru substrate was produced under the same preparation conditions. The results provide further insights into the factors that influence the formation of two-dimensional frameworks intended to be used as model systems for surface science studies of rigid porous materials.

KEYWORDS: Percolated network; zeolite model system; surface science; ultra-thin aluminosilicate clays; silicate films.

1. INTRODUCTION

The use of structure directing agents during the synthesis of zeolites is a well established method to tune the geometry of three-dimensional frameworks. [1] We have recently used a similar strategy to produce a two-dimensional framework. In that case, a flat metallic substrate was used as a template for the growth of a self-containing ordered aluminosilicate structure composed of a planar arrangement of hexagonal prisms, a.k.a. double 6-membered rings (*d6r*). [2] A depiction of the structure is shown in figure 1b. A similar structure was reported before for a film containing only Si atoms in the tetrahedral positions. [3] In addition, a layered material called hexacelsian, reported as early as 1951, [4] also has this structure as a part of each layer. Interestingly, the structure of hexacelsian is also formed when the framework of the most widely used zeolite, Zeolite A, in its Ba-exchanged form, collapses upon thermal treatment. [5] Due to the nature of this new class of two-dimensional frameworks, the set of analytical tools used to characterize them is different from the ones commonly used to study zeolites and related materials. For example, diffraction patterns to assess the long range order of these films are obtained by low energy electron diffraction (LEED), instead of X-ray diffraction. The tools used to study these films belong to the field of surface science, for which a whole plethora of analytical techniques is available. [6] This offers the possibility of using the two-dimensional structures to perform very detailed studies on systems that share many properties with the three-dimensional zeolite analogs. For example, scanning tunneling microscopy (STM), allows the visualization of the structure down to the atomic scale [7] and it even offers the possibility of doing spectroscopy at the single atom level. [8] There is no doubt that studying structures to this level of detail translates into significant progress towards the understanding of zeolites, and other solid catalysts, and this has been made evident in recent years by the visualization of structures at the nanoscale using electron microscopies. [9, 10] In addition, surface science studies allow the characterization of films in the extremely pristine conditions provided by ultra-high vacuum environments, down to 10^{-13} atm.

Needless to say, a significant difference of these films with three-dimensional zeolites is the lack of the rich variety of pores that are found in the latter. The only cavities present in the films are the small spaces contained within the hexagonal prisms and other, less frequently found, polygonal prisms. [7] However, the exposed surface of the film can be pictured as a pore of infinitely large size. In fact, we have demonstrated in a previous work that the same bridging hydroxyls found in acidic zeolites are present also in the two-dimensional films, [2] and that they behave in a similar way towards the adsorption of probe molecules CO, C_2H_4, NH_3 and pyridine. [11]

It was only recently that the preparation of silica and aluminosilicate ultra-thin films of well-defined structures was achieved. [12] Depending on the amount of Si and Al deposited during the film preparation, and the nature of the metallic substrate onto which the film was grown, it was found that monolayer or bilayer structures are produced. For clarity, we will now define a monolayer equivalent (MLE) as the amount of Si (or Al) necessary to produce the monolayer structure shown in figure 1a. Note that ordered structures for more than 2 MLE have not been reported yet.

While monolayer films are chemically bound to the metallic substrate through oxygen linkages Si—O—M, [13] the bilayer case is a self-containing structure (all atoms are bound only to other atoms in the framework) in which the two layers are bound together by Si—O—Si(Al) linkages, [3] and the interaction between the film and the substrate occurs through Van-der-Waals forces (see figure 1b). For example, for the case of crystalline silica films, only monolayers can be produced on Mo(112) [13] and only bilayers on Pt(111) [14]. For Ru(0001) both structures can be prepared depending on the amount of Si. Monolayers are obtained for 1 MLE of Si and bilayers are obtained for 2 MLE. Intermediate amounts of silicon give rise of films containing both monolayer and bilayer domains. [15] This was rationalized based on the affinity of oxygen to the metal support, which is reflected on the heats of dissociative adsorption of oxygen: Mo = −544 kJ/mol > Ru = −220 kJ/mol > Pt = −133 kJ/mol. [14] Since the Mo—O bond is so strong, a structure bound to the metal (monolayer) is thermodynamically more stable than one that is not (bilayer). The opposite is true for the Pt(111) case, for which the Pt—O bond is much weaker.

The aluminosilicate case is of prime importance to the zeolite community, since these films can be used to model some of the properties of zeolites using the versatile set of analytical tools available in surface science. On Mo(112) only monolayer films could be obtained and attempts to grow thicker ordered films were unsuccessful. [16] On Ru(0001), however, an aluminosilicate bilayer film consisting of SiO_4 and AlO_4^- tetrahedra was produced when 2 MLE of tetrahedral atoms T (Si or Al) were deposited.[2, 7] Both of these cases are in agreement with what is expected from the results of silica films.

While the micropores in the zeolite structure play a major role in housing the active sites and in granting size selective access to small molecules, the importance of mesoporosity in the catalytic activity of zeolite crystals is increasingly being recognized. Recently, studies on H-ZSM-5 suggested that most of the activity in zeolite catalysts happens near the surface and the active sites in the interior of the individual crystals remains inaccessible to the reactants. Only severe steaming treatments generated extensive mesoporosity allowing the whole crystal to be

accessible but at the cost of a significant loss in catalytic activity by depletion of active sites. [17] Since the presence of mesoporosity throughout the catalyst is beneficial to let bulky molecules go through to prevent blocking of the active sites, an alternative is the use of hierarchical zeolites which inherently contain mesopores in the structure, in addition to the micropores. An example of this is the use of three-dimensional arrangements of two-dimensional structures such as thin zeolite sheets to build more complex structures with channels in the mesopore scale. [18]

In the present work we report a case in which 0.9 MLE of T atoms (Si + Al) are deposited on Ru(0001) which, based on what was found for silica, should form a monolayer structure. However, we find that a percolated network with bilayer structure covering half of the surface is formed. Interestingly, the percolated network leaves voids with sizes in the mesoporous scale range, through which the Ru(0001) template is exposed.

2. EXPERIMENTAL

All experiments reported here were performed in an ultrahigh-vacuum (UHV) system (base pressure ~ 5×10^{-10} mbar) counting with the following techniques: x-ray photoelectron spectroscopy (XPS), infrared reflection absorption spectroscopy (IRAS), scanning tunneling microscopy (STM) and low energy electron diffraction (LEED). Silicon was deposited using an e-beam-assisted evaporator (Focus EFM3). During evaporation, the substrate was biased at the same potential as the Si rod (1000 V) to prevent acceleration of ions toward the sample, which could create uncontrolled defects. Aluminum was evaporated from a home-built evaporator consisting of a crucible containing metallic Al. The film was prepared on a Ru(0001) sample (10 mm in diameter and 1.5 mm in thickness from Mateck) surface which was first cleaned with cycles of Ar^+ sputtering (2kV, 15 μA) and annealing to ~1200 °C. The clean surface was then pre-covered with a 3O-(2 × 2) overlayer by exposing the crystal to 3×10^{-6} mbar O_2 at 950 °C. The aluminosilicate film was prepared by subsequently depositing ~ 0.57 MLE of Si and ~ 0.33 MLE of Al on the 3O-(2 × 2)/Ru(0001) surface under an O_2 pressure of 2×10^{-7} mbar. 1 MLE is defined as the number of T atoms (Si or Al) necessary to make 1 ML of the structure shown in Figure 1a. Note that 1 MLE corresponds to approximately 0.79×10^{15} T atoms/cm^2, this corresponds to 1 T atoms for every 2 Ru surface atoms. The composition of the film was confirmed by XPS. A correction factor of 1.17 was applied to the ratio of the peak areas Si 2p/Al 2s, based on previously reported experimental sensitivity factors. [19] This same procedure was followed our previous articles and it accounts for the difference in cross section of Si 2p and Al 2s core levels. [2,7,11] The film was then oxidized by

exposing it to a pressure of O_2 of 3×10^{-6} mbar while heating the sample up to ~ 950 °C, keeping it at this temperature for 10 minutes and then cooling it down always under O_2 ambient.

STM images were acquired with and Omicron ST Microscope at 300 K in the constant-current mode, with a current set-point of ~ 66 pA and bias voltage of - 0.7 V applied to the sample. Image processing was done with WSXM software. [20]

3. RESULTS

Figure 2a shows an STM image of the aluminosilicate film, where the area covered by the film can be clearly distinguished from the voids that leave the Ru(0001) surface exposed. The hexagonal structure from the six-membered rings of the framework can be distinguished as well in this image. To ease the visualization of the structure, the image was filtered using wavelet analysis [20] (with a wavelet scale of 0.05 nm) and this is shown in Figure 2b. Here it can be clearly seen that, in addition to a majority of 6-membered rings, other polygons are also found forming part of the structure, similar to what was found before for a bilayer structure covering the whole surface. The long range order is verified by LEED (Figure 3c) where both the (1 × 1) lattice of the Ru(0001) substrate, used as a reference, and the (2 × 2) lattice of the film can be seen in the diffraction pattern. The lattice constant of the Ru(0001) unit cell is 2.71 Å. A cartoon with the structure of the film, based on DFT calculations from the Sauer group, [2] is shown in figure 2d, where the unit cells of both the substrate and the film are shown. Note that the exact position of the aluminum atoms in the real structure could not be determined from the currently available data and therefore here we show arbitrarily chosen positions for Al. Low temperature scanning tunneling microscopy and spectroscopy studies are currently under way, aiming to determine precisely the location of the Al atoms in the framework.

An STM image for a much larger scale (200 nm × 200 nm) is shown in figure 3. Note that a step edge of Ru(0001) runs across the surface separating two terraces. A line profile (green line in the image) was taken through the terraces and going across the step edge. A plot of the profile is also shown in the figure (right). Here, the step height (~ 2 Å) can be clearly seen and it is in good agreement with the height expected from a step on the Ru(0001) surface. The approximate apparent height of the film with respect to Ru(0001) is ~ 4 Å, at the imaging conditions used here.

It can also be observed from the image that there is a continuity of the film across the step edge. A percolated network can be seen spanning across the surface and covering approximately half of the surface area. The remaining area corresponds to exposed Ru(0001) which is presumably partially covered by mobile adsorbates, as expected from

the time passed between preparation of the sample and image acquisition, which allows for background gasses, mostly CO, to adsorb on the exposed Ru crystal. An experimental indication of this is seen in the close-up area shown in the inset, showing streaky lines in the scanning direction (horizontal direction), which are only present on the area not covered by the aluminosilicate film (CO does not adsorb on the film in UHV). The size of the exposed Ru areas is in the scale range of mesopores.

The amount of Si, Al and O present on the surface, as well as their chemical state, was determined by XPS. Figure 4 shows XPS spectra of Si 2p, Al 2s and O 1s core levels for the 0.9 MLE aluminosilicate and 2 MLE films, with comparable Si/Al ratios, i.e.: 1.7 and 1.9 respectively. The Si 2p and Al 2s peaks are found at ~ 102.5 eV and ~ 118.7 eV respectively. The O1s peak can be deconvoluted into three contributions, depending on the environment of the O atom, at 531.7 eV, 530.7 eV and 529.9 eV, corresponding to Si—O—Si, Al—O—Si, and O—Ru respectively, based on previous assignments. [2, 21] Note that for the case of 2 MLE, the contribution of the oxygen located between Si atoms is higher than for the 0.9 MLE sample, due to the higher Si/Al ratio in the former case (1.9 as opposed to 1.7). Additionally, the O between Al and Si is expected to be attenuated with respect to the one between two Si atoms due to the fact that Al is preferentially located at the bottom layer of the bilayer (closer to the Ru substrate). This was speculated based on STM images and IRA spectra of bridging hydroxyl groups in a previous study [2] and confirmed later by energy and angle dependent XPS studies using synchrotron radiation. [22] Deconvoluted versions of the O 1s spectra are shown as supporting information, where a good fit is obtained when using the binding energies previously reported in the literature for the different O species present in this system. Note that in the case of the 0.9 MLE, the area of the surface that is not covered by the film could be potentially oxidized. However, at the conditions used here for the film preparation, only the formation of a 3O-(2 × 2) overlayer was reported. For other conditions that lead to the formation of ruthenium oxides, the reader is referred to reference [23].

Figure 5 shows the infrared reflection absorption spectrum for the 0.9 MLE film. There, a sharp high-frequency (HF) phonon vibration at 1264 cm^{-1} and a low-frequency one at 693 cm^{-1} can be observed. These are in the range corresponding to a bilayer structure and the phonon vibration modes assigned to these peaks are schematically shown in the figure.

4. DISCUSSION

It was previously found that silica films grown by deposition of 1 MLE of Si atoms on Ru(0001) cover the entire surface with the structure shown in figure 1a. It was then expected that a similar structure would be formed upon preparing a 1 MLE (or less) film in which some of the Si was replaced by Al. However, for the film reported in this work, for which 0.9 MLE of (Si + Al) atoms were deposited, as measured by XPS (see figure 4), STM images (figure 2) reveal that only about half of the surface was covered by the film, rather than the expected 90% of the surface. The amount of material present on the surface and the area covered by the film then seem to suggest that a bilayer structure was formed.

The most important piece of information to distinguish monolayer and bilayer structures comes from IRAS, since they both have very distinct spectral signatures. The bilayer structure has a strong high-frequency (HF) phonon vibration at 1300 cm^{-1} for pure-silica films and the frequency red-shifts, without losing intensity, when Si atoms are replaced by Al in the framework. For example, for a film with a composition $Al_{0.19}Si_{0.81}O_2$ (Si/Al = 4.3), the frequency of the HF mode shifts to 1281 cm^{-1}. [2] In contrast, for the monolayer silica on Ru(0001), this vibrational mode is not present. Instead two other modes appear in the spectrum at 1134 cm^{-1} and 1074 cm^{-1}. [15] Note that, for all films, other modes at lower frequencies (ranging from ~650 cm^{-1} to ~800 cm^{-1}) are also present in the spectrum, which will not be discussed here.

The observation of a high-frequency phonon vibration at 1264 cm^{-1}, associated with Si—O—Al (Si) oscillators normal to the surface, confirms that the bilayer structure (figure 1b) was formed, rather than the monolayer one. This accounts then for the coverage observed in the STM images. This behavior, the formation of bilayer structures regardless of the coverage of T atoms, was previously found for SiO_2 on Pt(111) surfaces. However, in the latter, vitreous films were obtained while in the present work the film is crystalline as confirmed by the observation of a hexagonal lattice by STM in figure 3, with a long range order confirmed by LEED (figure 2c). The order in this film can be rationalized based on the good lattice match between the aluminosilicate and the Ru(0001) substrate, and this was already observed in previous works, in which mostly hexagonal prisms (*d6r*) are observed in the film and, only for very high Al contents, other polygonal prisms are present on the surface. Note that the *d6r* building block is one of the most common ones as well for three-dimensional frameworks and there are 10 different framework types that can be built entirely using just *d6r*. [24] In fact, a closer look at figure 2 reveals the presence of other ring sizes, similar to the bilayer structure covering the whole surface. [7]

Another fact that becomes evident when comparing the IRAS data for this and full-bilayer films with similar Si/Al ratio is that, for the 0.9 MLE case, the frequency of the HF phonon vibration is slightly lower than expected. For comparison, for the 2 MLE film with Si/Al = 1.9 this phonon vibration is found at 1278 cm^{-1}. This indicates that the vibrational frequency does not only depend on the Si/Al ratio, but also decreases when the total coverage of tetrahedral atoms decreases. Additionally, the intensity of the peak for the 0.9 MLE film is approximately four times lower than that of the 2 MLE one.

The fact that monolayer structures are not formed can be explained considering results from previous works. For aluminosilicate films on Mo(112) it was shown that only the monolayer structure can be produced in an ordered manner. [16] However, in that case, Al—O—Mo linkages are not formed, which leaves the Al atoms bound to only three adjacent Si atoms in the plane through O-bridges, i.e.: the Al atom does not have tetrahedral coordination in this case. Nevertheless, the film is bound to the substrate through strong Si—O—Mo bonds which stabilize the structure. For the case reported here, under the assumption that Al—O—Ru linkages cannot be formed, the now reduced number of O—Ru bonds in the Si—O—Ru linkages is not strong enough to stabilize the structure, as it was for the Mo case. This can be rationalized base on the heats of dissociative adsorption of oxygen which are −544 kJ/mol for Mo and −220 kJ/mol for Ru. [14] While for the case of monolayer SiO_2 on Ru(0001) there are 2.0 Si—O—Ru linkages per unit cell, for a monolayer aluminosilicate with the composition reported here (37% Al), there would be ~ 1.35 Si—O—Ru linkages per unit cell. On the other hand, it was previously shown that the bilayer structure does stabilize Al with tetrahedral coordination. [2]

While for the purpose of preparing model systems the influence of the metallic substrate should be minimized, it results evident from this and previous studies that, [14] even in the cases in which the interaction is through Van-der-Waals forces, the substrate has a strong role in the type of structures that can be prepared. The factors that determine the growth mode are: 1) the interaction and 2) the registry between the film and the substrate. In the case reported here, the substitution of some Si atoms by Al has an influence in both of these factors. The interaction with the films is strongly affected since, for the monolayer structure, a reduction in the number of oxygen-metal bonds is expected, considering that Al does not form Al—O—M linkages. In terms of the registry, it is useful to consider the lattice constant for a free-standing silica bilayer structure, which was computed to be 5.32 Å. [25] When the silicate bilayer is grown on Ru(0001), the relatively “weak” interaction with the substrate is evidently strong enough to induce an expansion of the framework lattice to 5.42 Å, to be in registry with (2 ×) the unit cell (2.71 Å) of Ru(0001). In fact, this

is not always true, and it was often found that vitreous structures coexist with the crystalline ones for this case. [15] For a framework containing Al, however, there are two factors that favor a better adaptation of the framework to the Ru(0001) lattice. First, since the Al—O bond is less covalent than the Si—O bond, there is more flexibility in the O—T—O and T—O—T angles. [26-28] This has an influence in the distance between the T atoms in the framework, providing more flexibility to the framework to adapt to external forces, such as the interaction with the Ru(0001) template. Second, the Al—O bond (1.70 Å – 1.73 Å) is longer than the Si—O bond (1.58 Å – 1.64 Å), [26] also favoring an expansion of the lattice when compared to the pure-silica case, providing a better match with the Ru(0001) lattice.

Another interesting feature of this film, in terms of topology, is the formation a percolated network which leaves irregularly shaped voids in the structure of sizes in the mesoscale range. This is structurally analogous, although in the two-dimensional case, to what was observed for ZSM-5 subjected to dealumination by a severe steaming treatment. [17] Using atomic force microscopy and high-resolution scanning electron microscopy of individual ZSM-5 crystals, it was found that uniformly distributed mesopores between 5 nm and 50 nm are present in the structure.

A bilayer film which is not chemically bound to the metallic substrate is much more useful as a model system for the three-dimensional porous materials than the strongly bound monolayer case. In particular, films that also count with mesoporosity, such as the one reported here, could be used for modeling features found in some cases of dealuminated zeolites. In addition, the mesoporous voids can be used for hosting catalytically active nanoparticles. This would provide then a model system for bifunctional catalysts in which both, the zeolite and the nanoparticle, participate in the reaction. An example of this is the case of Ru particles on mesoporous beta zeolite to catalyze the conversion of synthesis gas to hydrocarbons (Fischer–Tropsch synthesis), [29] for which this film would be ideal since Ru is already present in the voids.

5. CONCLUSIONS

A self-containing ultra-thin (~ 0.5 nm) aluminosilicate farmework covering approximately half of a surface was synthesized using Ru(0001) as a template. It is composed mostly of hexagonal prisms as building blocks and it forms a percolated network leaving the ruthenium substrate exposed through irregularly shaped voids in the mesopore scale range. The bilayer structure of the film is different from what was previously found for films prepared in the same manner but without Al in the framework, which form monolayer silicate films strongly bound to the substrate. This

difference is rationalized based on the reduced number of Si—O—Ru linkages, if a monolayer was formed, when Al is incorporated in the framework. The incorporation of Al also favors more crystalline frameworks and this is related to a better lattice match between the film and the Ru(0001) template as well as to the less covalent character of Al—O bonds when compared to Si—O bonds.

ACKNOWLEDGMENT

J.A. Boscoboinik gratefully acknowledges a fellowship by the Alexander von Humboldt Foundation.

REFERENCES

[1] Z. Wang, J. Yu, R. Xu, Chem. Soc. Rev., 41 (2012) 1729-1741.
[2] J.A. Boscoboinik, X. Yu, B. Yang, F.D. Fischer, R. Włodarczyk, M. Sierka, S. Shaikhutdinov, J. Sauer, H.-J. Freund, Angew. Chem. Int. Ed., 51 (2012) 6005-6008.
[3] D. Löffler, J.J. Uhlrich, M. Baron, B. Yang, X. Yu, L. Lichtenstein, L. Heinke, C. Büchner, M. Heyde, S. Shaikhutdinov, H.-J. Freund, R. Wlodarczyk, M. Sierka, J. Sauer, Phys. Rev. Lett., 105 (2010) 146104.
[4] B. Yoshiki, K. Matsumoto, J. Am. Ceram. Soc., 34 (1951) 283–286.
[5] J. Djordjevic, V. Dondur, R. Dimitrijevic, A. Kremenovic, Phys. Chem. Chem. Phys., 3 (2001) 1560-1565.
[6] D.P. Woodruff, T.A. Delchar, Modern Techniques of Surface Science, 2nd edition ed., Cambridge University Press, Cambridge, 1994.
[7] J.A. Boscoboinik, X. Yu, B. Yang, S. Shaikhutdinov, H.-J. Freund, Microporous Mesoporous Mater., 165 (2013) 158-162.
[8] N. Nilius, Surf. Sci. Rep., 64 (2009) 595-659.
[9] I. Diaz, A. Mayoral, Micron, 42 (2011) 512-527.
[10] J.M. Thomas, P.A. Midgley, ChemCatChem, 2 (2010) 783-798.
[11] J.A. Boscoboinik, X. Yu, E. Emmez, B. Yang, S. Shaikhutdinov, F.D. Fischer, J. Sauer, H.-J. Freund, J. Phys. Chem. C, 117 (2013) 13547–13556.
[12] S. Shaikhutdinov, H.-J. Freund, Adv. Mater., 25 (2013) 49-67.
[13] J. Weissenrieder, S. Kaya, J.-L. Lu, H.-J. Gao, S. Shaikhutdinov, H.-J. Freund, M. Sierka, T.K. Todorova, J. Sauer, Phys. Rev. Lett., 95 (2005) 0761031.
[14] X. Yu, B. Yang, J.A. Boscoboinik, S. Shaikhutdinov, H.-J. Freund, Appl. Phys. Lett., 100 (2012) 151608-151604.
[15] B. Yang, W.E. Kaden, X. Yu, J.A. Boscoboinik, Y. Martynova, L. Lichtenstein, M. Heyde, M. Sterrer, R. Wlodarczyk, M. Sierka, J. Sauer, S. Shaikhutdinov, H.-J. Freund, Phys. Chem. Chem. Phys., 14 (2012) 11344-11351.
[16] D. Stacchiola, S. Kaya, J. Weissenrieder, H. Kuhlenbeck, S. Shaikhutdinov, H.-J. Freund, M. Sierka, T.K. Todorova, J. Sauer, Angew. Chem. Int. Ed., 45 (2006) 7636-7639.
[17] L.R. Aramburo, L. Karwacki, P. Cubillas, S. Asahina, D.A.M. de Winter, M.R. Drury, I.L.C. Buurmans, E. Stavitski, D. Mores, M. Daturi, P. Bazin, P. Dumas, F. Thibault-Starzyk, J.A. Post, M.W. Anderson, O. Terasaki, B.M. Weckhuysen, Chem. Eur. J., 17 (2011) 13773-13781.
[18] X. Zhang, D. Liu, D. Xu, S. Asahina, K.A. Cychosz, K.V. Agrawal, Y. Al Wahedi, A. Bhan, S. Al Hashimi, O. Terasaki, M. Thommes, M. Tsapatsis, Science, 336 (2012) 1684-1687.
[19] C.D. Wagner, L.E. Davis, M.V. Zeller, J.A. Taylor, R.H. Raymond, L.H. Gale, Surf. Interface Anal., 3 (1981) 211-225.

[20] I. Horcas, R. Fernandez, J.M. Gomez-Rodriguez, J. Colchero, J. Gomez-Herrero, A.M. Baro, Rev. Sci. Instrum., 78 (2007) 013705.
[21] J.A. Boscoboinik, X. Yu, B. Yang, F.D. Fischer, R. Włodarczyk, M. Sierka, S. Shaikhutdinov, J. Sauer, H.-J. Freund, Angew. Chem., 124 (2012) 6107-6111.
[22] J.A. Boscoboinik, E. Emmez, X. Yu, B. Yang, B.-H. Liu, S. Shaikhutdinov, H.J. Freund, In Preparation.
[23] Y. Martynova, B. Yang, X. Yu, J.A. Boscoboinik, S. Shaikhutdinov and H.-J. Freund, Catal. Lett. 142 (2012) 657-663.
[24] C. Baerlocher, L.B. McCusker, Database of zeolite structures, www.iza-structure.org/databases2007.
[25] U. Martinez, L. Giordano, G. Pacchioni, J. Phys. Chem. B, 110 (2006) 17015-17023.
[26] R.F. Lobo, Introduction to the structural chemistry of zeolites, in: S.M. Auerbach, K.A. Carrado, P.K. Dutta (Eds.) Handbook of Zeolite Science and Technology, Marcel Dekker, New York, 2003.
[27] W. Depmeier, Structural distortions and modulations in microporous materials, in: H.G. Karge, J. Weitkamp (Eds.) Molecular Sieves: Science and Technology, Springer-Verlag, Berlin, 2001, pp. 113-129.
[28] W. Depmeier, Acta Crystallogr., Sect. C, 40 (1984) 226-231.
[29] K. Cheng, J. Kang, S. Huang, Z. You, Q. Zhang, J. Ding, W. Hua, Y. Lou, W. Deng, Y. Wang, ACS Catal., 2 (2012) 441-449.

Figure Captions

Figure 1. Top and side views of (a) monolayer and (b) bilayer structures on a metal support. T stands for tetrahedral atoms (Si or Al).

Figure 2. a) High-resolution STM image where the aluminosilicate network and the voids exposing Ru(0001) can be seen. b) Filtered version of image a) using wavelet analysis; the inset at the lower right-hand corner shows the (2 × 2) unit cell of the film . c) Low energy electron diffraction pattern, where the (2 × 2) spots of the film and the (1 × 1) Ru(0001) substrate spots can be clearly seen. d) Representation of the film structure where the film and substrate unit cells are emphasized.

Figure 3. Top: large scale STM image (200 nm × 200 nm) showing the film forming a percolated network. The inset shows a higher resolution image where streaky lines can be seen in the voids in the direction of the motion of the scanning tip (horizontal direction). Bottom: line profile going along the green line shown in the image. The left side of the profile corresponds to the bottom left part of the image. A height of ~ 2 Å can be seen at ~ 120 nm, corresponding

to an atomic step of the Ru(0001) surface. The ~ 4 Å amplitude comes from the difference in apparent height between the framework and the Ru(0001) surface.

Figure 4. XPS spectra of the Al 2s, Si 2p and O 1s core levels for the film described here (0.9 MLE) and for a 2 MLE film used as a reference.

Figure 5. IRAS spectrum of the 0.9 MLE framework. The vibrational modes are shown schematically next to the peak.

Figure1.tif
Click here to download high resolution image

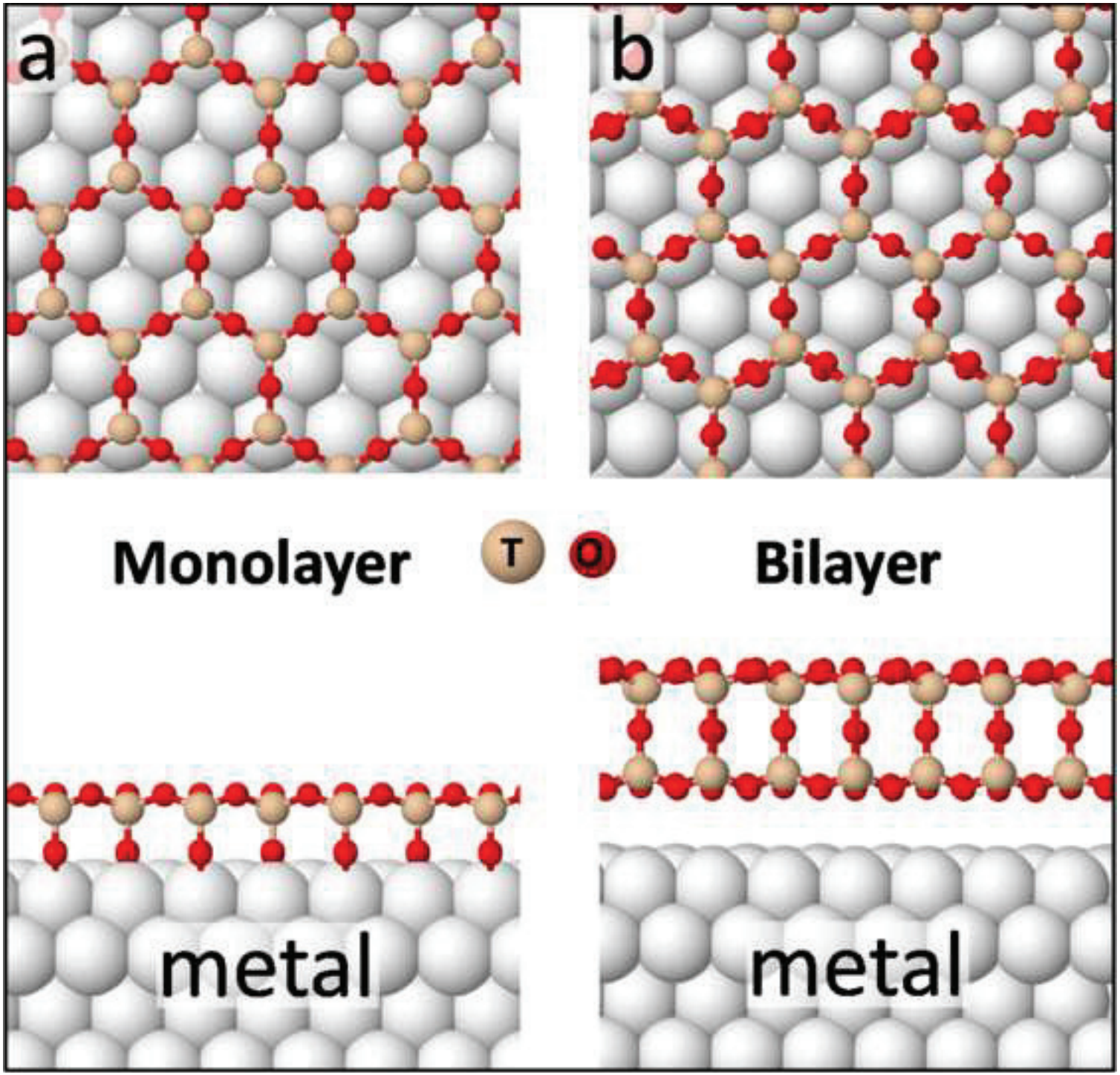

Figure2.tif
Click here to download high resolution image

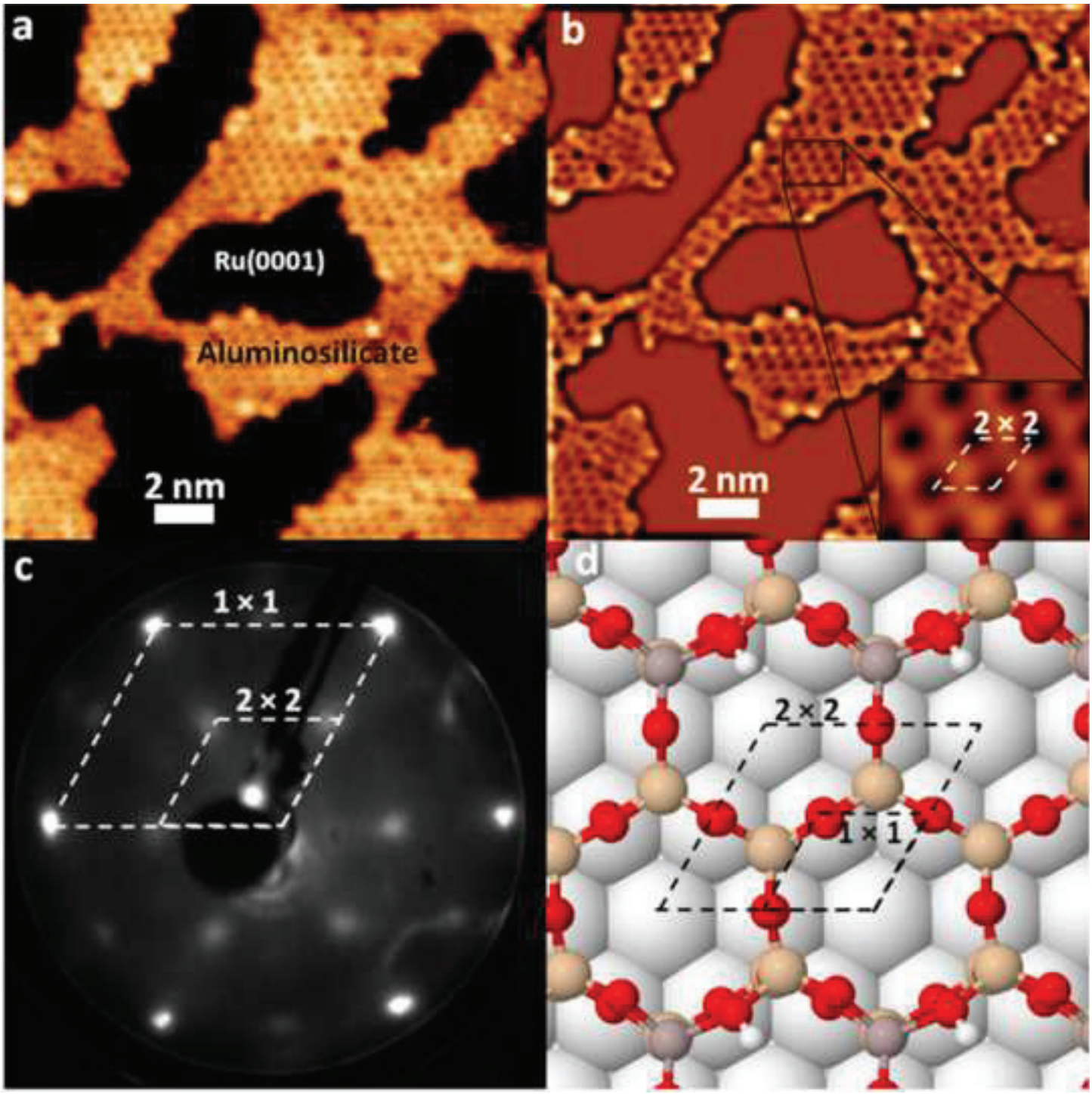

Figure3.tif
Click here to download high resolution image

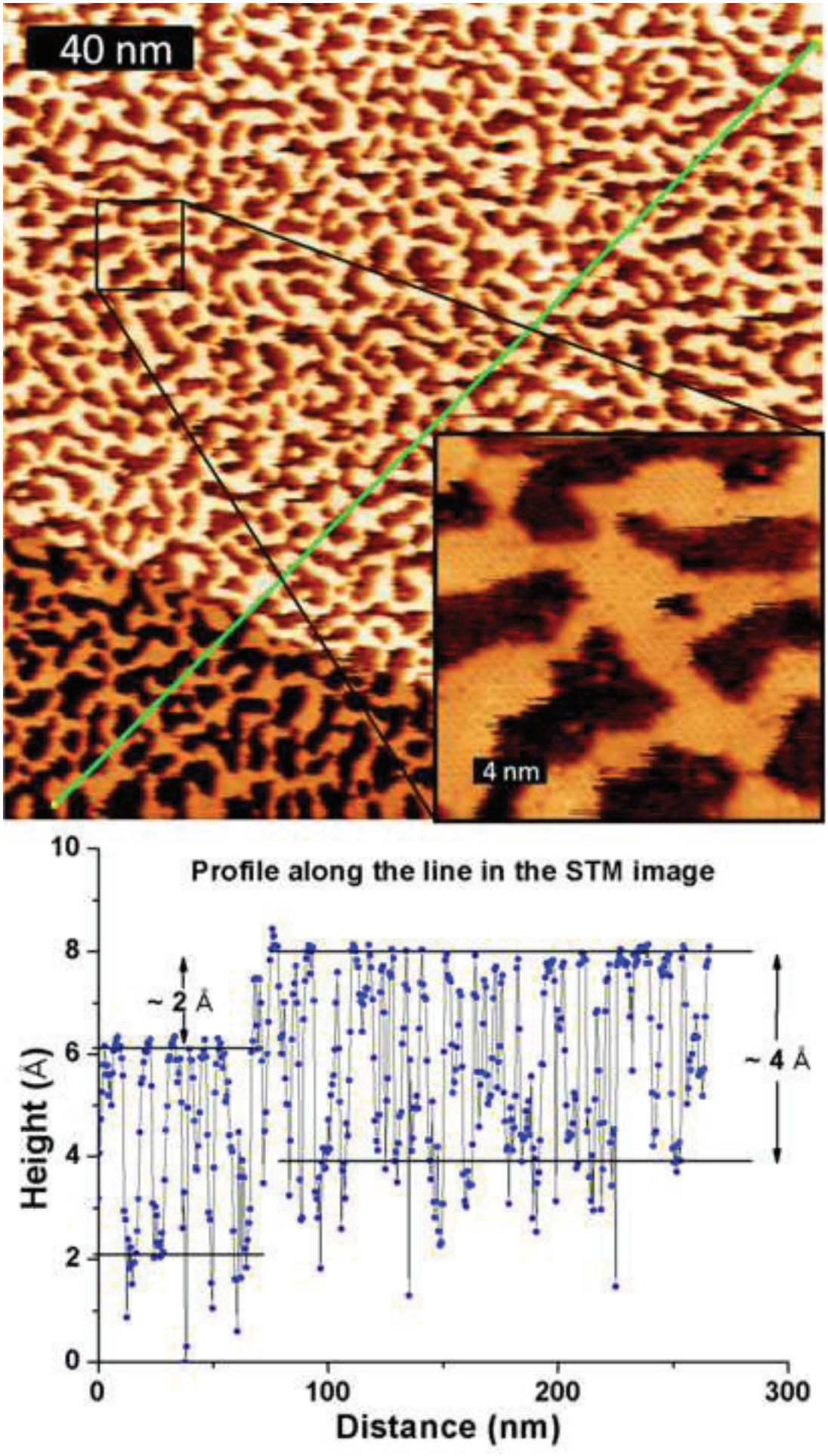

Figure4.tif
Click here to download high resolution image

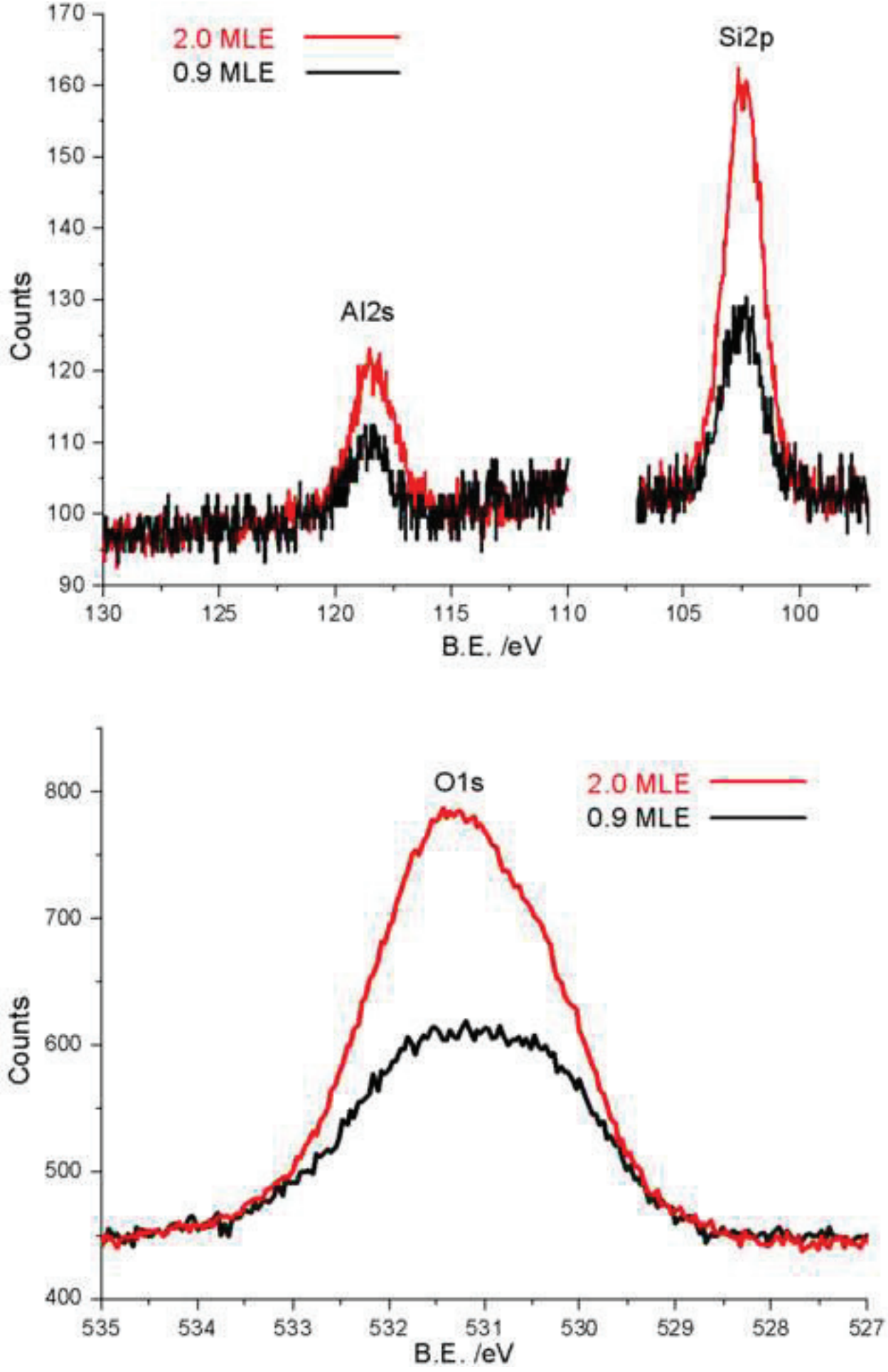

Figure5.tif
Click here to download high resolution image